

Chord intercepts in a two-dimensional cell growth model

Part 1 *Chord intercepts of the diminishing phase*

G. E. W. SCHULZE, H.-P. WILBERT

Abteilung Werkstoffwissenschaft des Instituts für Physik der Kondensierten Materie der Universität Düsseldorf, West Germany

Nuclei are Poisson-distributed within a plane. Out of the nuclei, grains begin to grow instantaneously, circularly and at a constant rate. The forming microstructure at each fraction transformed, consisting of grains and untransformed regions, is characterized in this work by use of a straight line (Rosin's line), which passes arbitrarily through the plane. Along this line we obtain chord intercepts of grains and of untransformed regions of different lengths, independent of the position of the straight line. The distributions of these lengths are essentially determined by the distribution of the nuclei and from the conditions of growth. From these assumptions we derive, by use of probability theory, the distributions of the chord intercepts. In Part 1, only the distribution density of the chord intercept of the untransformed regions is studied. From these results several other statistical quantities of the microstructure are also deduced.

1. Introduction

1.1. The problem

Fig. 1a shows circular grains of β -material, which grow into the supercooled α -material. Figs 1a to d show a chronological series of the same cut during the transformation of α to β . From Figs 1a to d we may abstract a good approximation of results. The centres (nuclei) of the circles are randomly distributed. (In Part 4 of this series we show experimentally, that the nuclei are Poisson-distributed, representing a special and exactly defined form of "random distribution".) The growth fronts α/β are circular and all exhibit the same radius $R = Gt$, where G is the radial growth rate and t the time of growth. The grain boundaries β/β are straight. During transformation no new nuclei are formed. Finally, at $t \rightarrow \infty$, only grains exist. This final microstructure is called the "cell model" [1] or "Voronoi tessellation" [2, 3]. Figs 1a to d are microphotographs obtained by unpolarized transmission light. The foil used is isotactic polypropylene with a thickness of about $4 \mu\text{m}$ during the transformation from the amorphous state (α) to spherulitic grains (β) at 133°C after cooling from about 200°C [4-6]. As β -grain is a "spherulite of type 1" [7] of the isotactic polypropylene and it is "partially crystalline" with a monoclinic crystal structure.

We restrict our investigations of the microstructure to linear analysis only [8-10]. Therefore, we characterize the microstructure only along an arbitrary straight line. Along this "Rosin's line" we see, in Figs 1a to d.

(i) α -chord intercepts of the amorphous phase with the random length a ;

(ii) β -chord intercepts of the grains with the random length b ;

(iii) γ -chord intercepts of transformed regions with the random length c , which are limited on both sides by α and which can contain grain boundaries β/β .

1.2. The aims

Using probability theory, we derive for the given model the cumulative distribution functions $A(a; t)$, $B(b; t)$, $C(c; t)$ of the lengths a , b , c of chord intercepts at time t , as well as their distribution densities $A'(a; t)$, $B'(b; t)$, $C'(c; t)$, respectively. (The derivation of the cumulative distributions A , B and C are given in Parts 1, 2, and 3, respectively.) From these results several other quantities of the microstructure are also derived.

In Part 4 it will be shown that these microstructures are realized within an amorphous foil of isotactic polypropylene. The experimental results are compared with the theoretical assumptions and results.

2. Derivation of the distribution density $A'(a; t)$

2.1. Definition of the microstructure at time t

The process forming the microstructure of the cell growth model in two dimensions at time t is given by the following conditions.

(i) Nuclei are Poisson-distributed in an infinite plane with a mean number, n , of nuclei per area unit.

(ii) Out of these nuclei the grains start to grow at $t = 0$ instantaneously and circularly with the same constant radial growth rate, G , and without shrinking. No new nuclei are formed during the process.

(iii) Wherever two growing grains touch, growth stops and necessarily these points form a straight grain boundary.

We note that equally distributed points in a finite

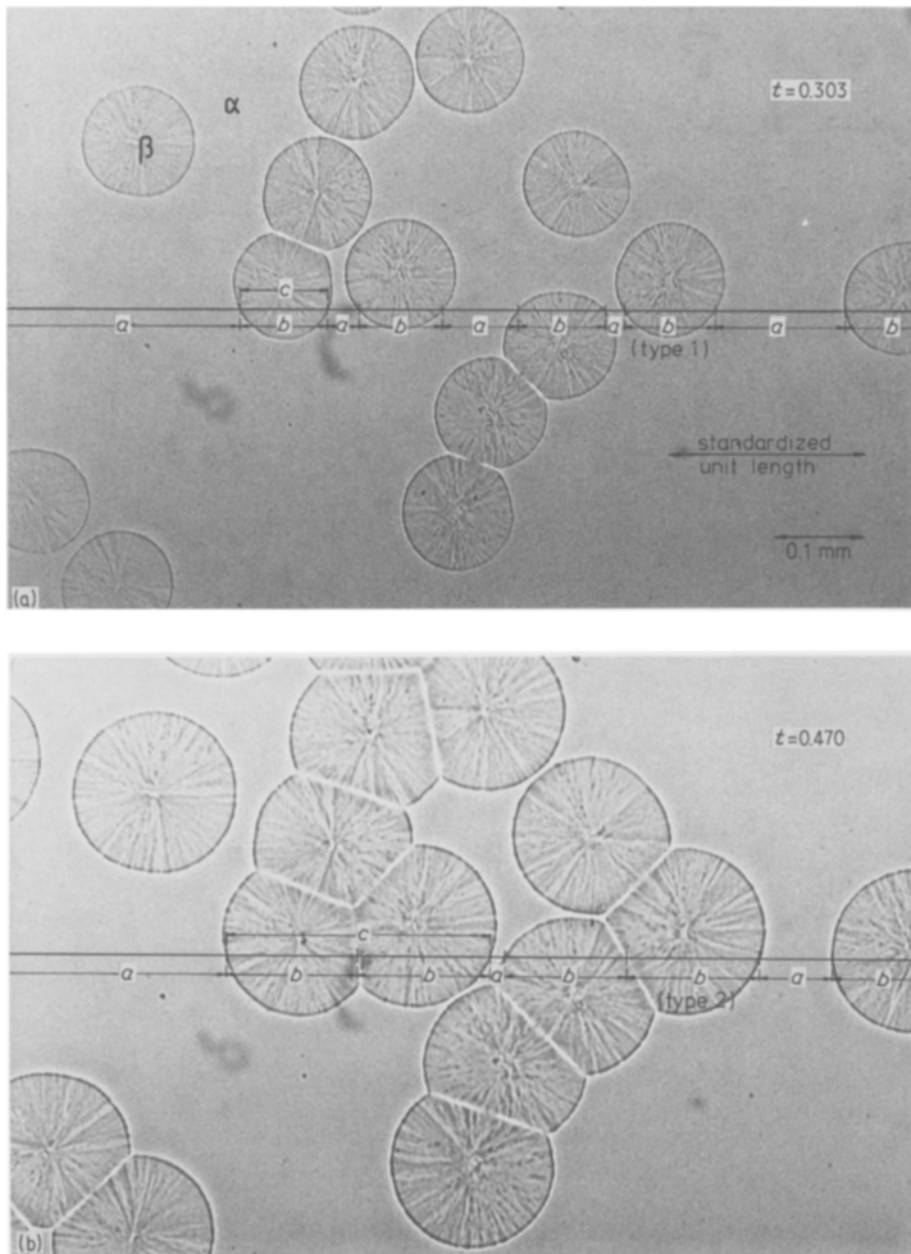


Figure 1 (a) to (d) Microstructures at four different times, (a) $t_1 = 0.303$; (b) $t_2 = 0.470$; (c) $t_3 = 0.664$. (d) $t_4 \rightarrow \infty$, in standardized units, corresponding to the four fractions transformed ($F = 1/4, 1/2, 3/4, 1$) of the same cut of the foil. Along Rosiwal's line (in the middle of the micrographs) we obtain chord intercepts of the random length a through α , of the random length b through grains, and of the random length c through transformed regions being limited on both sides by α . The chord intercepts of the grains are classified into three types: type 1, limited on both sides by α ; type 2, limited by α and β ; type 3, limited on both sides by β .

plane are Poisson-distributed in the limiting case of an infinite plane with the same mean number, n , of points per unit area. Poisson proved [11] that if we place arbitrarily a test area of extent S into a plane where points are Poisson-distributed with parameter n , then the probability, P_0 , of obtaining no point within S amounts to

$$P_0 = \exp(-H) \quad (1)$$

where

$$H = nS \quad (2)$$

Equation 1 is Poisson's formula in its simplest form [12]. H represents the mean number of points within the test area, S .

2.2. Avrami relation

The probability that a circle with radius $r = Gt$ contains no nucleus amounts to

$$P_{\text{circle}} = \exp[-n\pi(Gt)^2] \quad (3)$$

The mean point, M , of this unoccupied circle is located within α , because the outer nuclei cannot reach M with their grains until time t . Therefore, P_{circle} also gives the fraction of the α -area to the whole area, and

$$\begin{aligned} F(t) &= 1 - P_{\text{circle}} \\ &= 1 - \exp[-n\pi(Gt)^2] \end{aligned} \quad (4)$$

gives the fraction of the transformed β -area to the whole area. $F(t)$ is the fraction transformed and

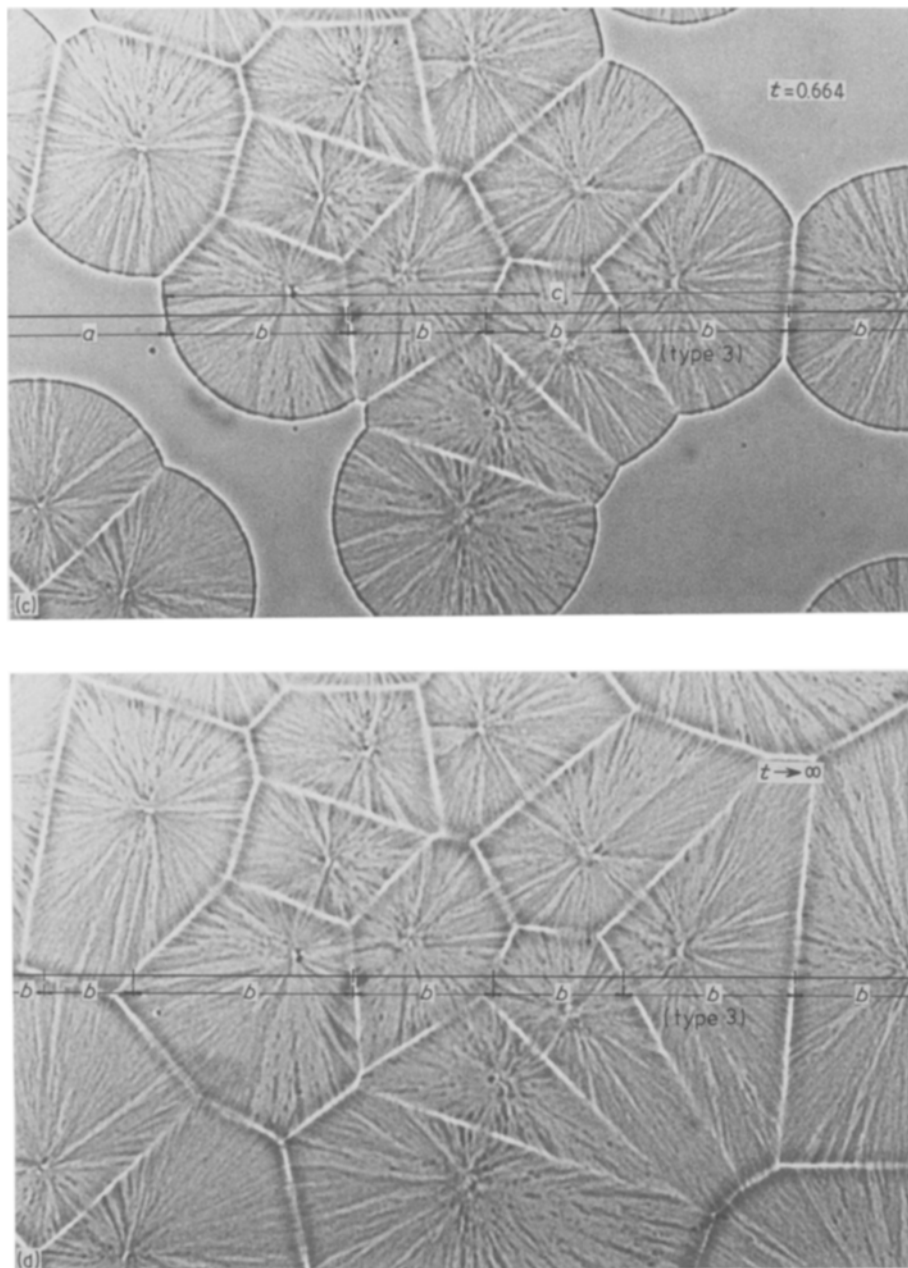


Figure 1 Continued

Equation 4 represents the well known Avrami relation of the model concerned.

The over-all kinetics runs with the rate of transformation, $f(t)$, given by

$$\begin{aligned} f(t) &= dF/dt \\ &= 2n\pi G^2 t \exp(-n\pi G^2 t^2) \end{aligned} \quad (5)$$

As shown in Fig. 2, $f(t)$ reaches its maximum at

$$t_{\max} = 1/[G(2n\pi)^{1/2}] \quad (6)$$

We physically interpret the shape of $f(t)$: at the beginning of the process the circles are very small and they do not touch each other. In this microstructure the rate of transformation increases nearly linearly, because the increase amounts to $2\pi R dR$ for a fixed dR and $R = Gt$. Later, grains stop growing by forming grain boundaries and finally many grains become full-grown. For $t > t_{\max}$ the latter effect dominates, as seen in Fig. 1c.

Note that it is possible to eliminate the two parameters n and G by introducing a new normalized length unit and a new normalized time unit. We use these new units in all following figures.

2.3. Distribution density $A'(a;t)$

Each arbitrary straight line through the microstructure of the cell growth model represents a Rosiwal-line and yields the same distributions of a , b and c , because the model of interest is statistically invariant of translation and rotation.

Fig. 3 shows Rosiwal's line in the middle of a band with a width of $2Gt$. Obviously at time, t , each nucleus within the band has reached Rosiwal's line with its grain, if unhindered growth is assumed. In contrast, each nucleus outside the band cannot reach Rosiwal's line with its grain.

Now we consider a nucleus N in Fig. 3 and its grain at time t , cutting Rosiwal's line at point O , where the a -interval of interest starts on the right side. In order

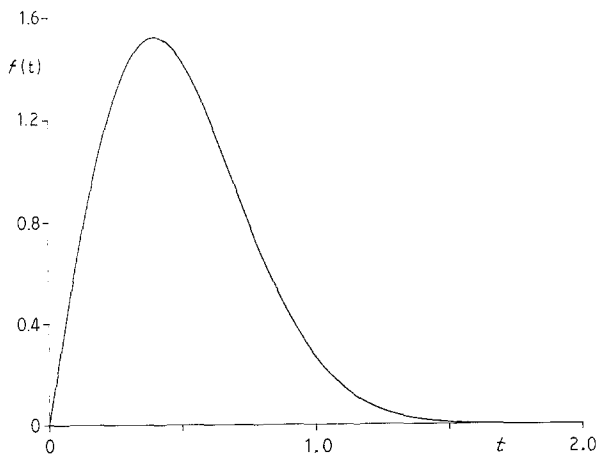


Figure 2 Rate of transformation, $f(t)$, with time, t , in standardized units. This curve represents three further quantities up to constant factors: the mean length of the growth front per unit area, S_A (Equation 21); the mean number, N_A , of α -chord intercepts per unit length along Rosiwal's line (Equation 15); and the mean number of growth fronts α/β per length unit along Rosiwal's line (Equation 16).

that O represents the left end of this a -interval, a circular area (shaded in Fig. 3) around O with radius Gt has to contain no nucleus, and only one nucleus, N, exists on its left arc. This condition may be satisfied as follows.

The length, a , on Rosiwal's line in Fig. 3 is completely arranged within α , if the left half circle around O, the rectangle with the area $2Gta$, and the right half circle around O' contains no nucleus. The probability that the rectangle contains no nucleus, is given by

$$P_{\text{rectangle}} = \exp(-2Gtna) \quad (7)$$

An α -chord intercept with a length $x > a$ and starting at O has to contain this length a . Therefore, $P_{\text{rectangle}}$ is also the probability for which $x > a$, and so the probability, that $x \leq a$, is given by

$$P(x \leq a) = 1 - P_{\text{rectangle}} \quad (8)$$

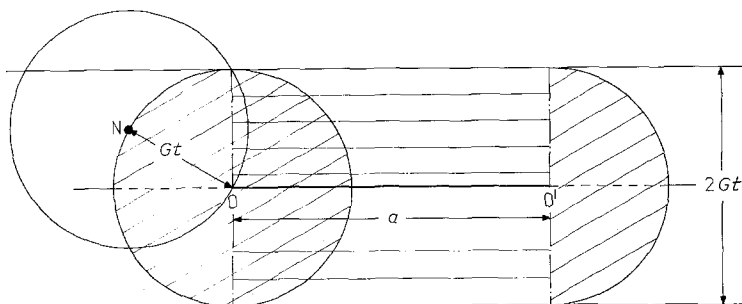
This probability is identical with the sought cumulative distribution function of length a at time t along Rosiwal's line, $A(a; t)$, as defined in probability theory

$$A(a; t) = 1 - \exp(-2nGta) \quad (9)$$

for $a \geq 0$ and $t > 0$

The corresponding distribution density amounts to

$$A'(a; t) = dA(a; t)/da = 2nGt \exp(-2nGta) \quad (10)$$



Of course, this distribution density is normalized:

$$\int_{a=0}^{\infty} A'(a; t) da = 1 \quad \text{for } 0 < t \quad (11)$$

We see that in each microstructure of the cell growth model in two dimensions, the lengths a of α -chord intercepts are exponentially distributed. A generalization has been given by Schulze [13], using another mathematical approach. A simulative verification of $A'(a; t)$ by use of more than 10^7 grains on Rosiwal's line has been given by Schwan *et al.* [14].

3. Consequences for the linear analysis

We obtain the following consequences along Rosiwal's line from the results above.

(a) $F(t)$ of Equation 4 is also the fraction transformed along Rosiwal's line. Therefore, $F(t)$ is also the mean transformed length per unit length at time t . Analogously, $1 - F(t)$ is the mean length of α per unit length at t .

(b) $f(t)$ of Equation 5 is also the rate of transformation along Rosiwal's line. Furthermore, it is the "mean rate of transformation per unit length", because $f(t)$ is an intensive quantity.

(c) The mean length, \bar{a} , follows from

$$\begin{aligned} \bar{a}(t) &= \int_{a=0}^{\infty} a A'(a; t) da \\ &= 1/(2nGt) \end{aligned} \quad (12)$$

We see that $\bar{a}(t)$ hyperbolically decreases with time, t , because more and more grains reach Rosiwal's line. (In the one-dimensional cell growth model, $\bar{a}(t)$ remains constant during the whole process [15].)

(d) The mean number, N_A , of α -chord intercepts per unit length follows from

$$N_A \bar{a}(t) = 1 - F(t) \quad (13)$$

We obtain

$$N_A(t) = 2nGt \exp(-n\pi G^2 t^2) \quad (14)$$

A simulative verification of $N_A(t)$ by use of more than 10^7 grains on Rosiwal's line has been given by Schwan *et al.* [14].

A comparison between Equations 5 and 14 yields

$$f(t) = \pi G N_A(t) \quad (15)$$

We see that $N_A(t)$ has the same shape as $f(t)$.

(e) The mean number of growth fronts α/β per unit length, N_{mov} , amounts to $2N_A$, because each γ -chord intercept grows on both sides. With this result we obtain from Equation 15

$$f(t) = (\pi/2) G N_{\text{mov}}(t) \quad (16)$$

Figure 3 Contribution to areas for derivation of $A(a; t)$. Around the nucleus, N, a grain with radius Gt exists, cutting Rosiwal's line at point O; O is starting point of an α -chord intercept, if the circular area around O with radius Gt contains no nucleus besides N. In order that the length a is completely arranged within α , we transfer the right half circle along length a from O to O'. The covered area amounts to $2Gta$, and this, too, must contain no nucleus.

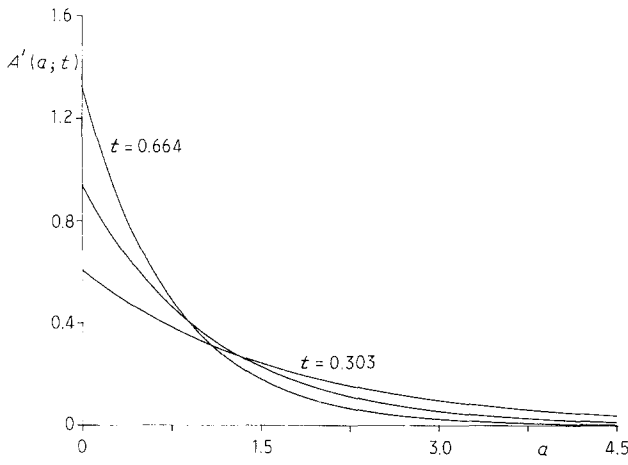


Figure 4 Distribution density, $A'(a; t)$ of the length a of α -chord intercepts at $t = 0.303, 0.470, 0.664$, corresponding to $F = 1/4, 1/2, 3/4$ respectively.

Obviously, the mean growth rate, \bar{v} , with which the γ -chord intercepts grow in both directions, amounts to

$$\bar{v} = (\pi/2)G \quad (17)$$

We see that \bar{v} is constant during the whole process.

(f) The mean length, $\bar{c}(t)$, of γ -chord intercepts along Rosiwal's line follows from

$$\bar{c}/\bar{a} = F/(1 - F) \quad (18)$$

and we obtain

$$\bar{c}(t) = [\exp(+n\pi G^2 t^2) - 1]/(2nGt) \quad (19)$$

$\bar{c}(t)$ increases monotonically with time t .

As shown in the following three points, the results above additionally lead to quantities being related to a unit area.

(g) The mean specific boundary, S_A is defined by the mean length of the growth fronts α/β per unit area. The increase, dF , of the transformed area per area unit between time t and $t + dt$ is given by

$$dF = S_A G dt \quad (20)$$

From Equations 5 and 15 we obtain

$$\begin{aligned} S_A &= (1/G)f(t) \\ &= 2n\pi Gt \exp(-n\pi G^2 t^2) \\ &= \pi N_A \end{aligned} \quad (21)$$

We see that $S_A(t)$ has the same shape as $f(t)$ and as $N_A(t)$.

(h) The mean relative specific boundary of α , $S_{A\alpha}$, is defined by S_A per fraction untransformed

$$S_{A\alpha} = S_A/(1 - F) \quad (22)$$

We obtain with Equations 20 and 14

$$S_{A\alpha} = \pi 2nGt \quad (23a)$$

$$= \pi/\bar{a} \quad (23b)$$

We see, that a linear relation exists between $S_{A\alpha}$ and t .

(i) The mean relative specific boundary of β , $S_{A\beta}$, follows analogously by

$$S_{A\beta} = S_A/F \quad (24a)$$

$$= 2n\pi Gt/[\exp(+n\pi G^2 t^2) - 1] \quad (24b)$$

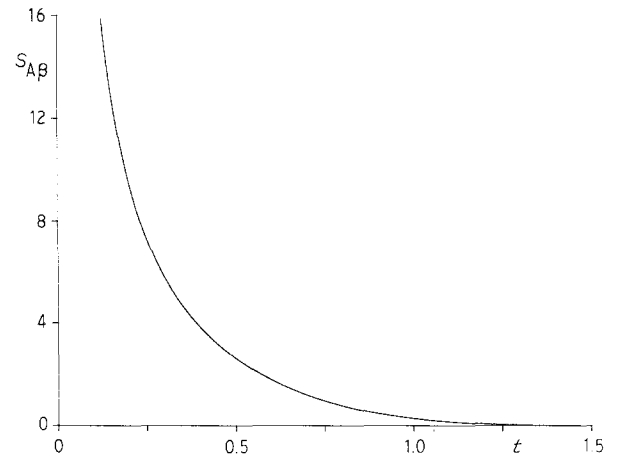


Figure 5 The dependence of the mean relative boundary of β , $S_{A\beta}$, on time, t .

$$= \pi/\bar{c} \quad (24c)$$

Fig. 5 shows the graph $S_{A\beta}(t)$.

In the field of quantitative microscopy the Equations 22, 23b and 24c are derived for more general two-dimensional microstructures by use of geometry and not of kinetics.

4. Conclusion

After a duration, t , of growth with the assumptions of the two-dimensional cell model, the following points are known:

1. Concerning the whole system:
 - the fraction of the transformed area, $F(t)$;
 - the fraction of the untransformed area, $1 - F(t)$;
 - the rate of transformation, $f(t)$;
 - the mean specific boundary, $S_A(t)$;
 - the mean relative boundary of α , $S_{A\alpha}(t)$;
 - the mean relative boundary of β , $S_{A\beta}(t)$.
2. along Rosiwal's line:
 - the transformed length, $F(t)$;
 - the untransformed length, $1 - F(t)$;
 - the rate of transformation, $f(t)$;
 - the distribution density, $A'(a; t)$, of the length a of untransformed intervals;
 - the mean length, $\bar{a}(t)$, of the untransformed intervals;
 - the mean length, $\bar{c}(t)$, of the transformed intervals;
 - the mean rate, \bar{v} , of the growth fronts.
3. per unit length along Rosiwal's line:
 - the mean transformed length, $F(t)$;
 - the mean untransformed length, $1 - F(t)$;
 - the mean rate of transformation, $f(t)$;
 - the mean number of untransformed intervals, $N_A(t)$;
 - the mean number of growth fronts, $N_{\text{mov}}(t)$.

Acknowledgements

We thank Dr L. O. Schwan, Dipl. Phys. L. Grutesen and Dipl. Phys. W. Weger for simulative verification of $N_A(t)$ and $A'(a; t)$ for some values of t . Dr R. Willers is thanked for discussion, Dr F. Kloos (Hoechst AG, Frankfurt/M.) for supplying the foil used in Figs 1a to d, and Miss H. Bickeböllner for smoothing of the translation.

References

1. J. L. MEIJERING, *Philips Res. Rep.* **8** (1953) 270.
2. A. L. HINDE and R. E. MILES, *J. Statist. Comput. Simul.* **10** (1980) 205.
3. H. G. HANSON, *J. Statist. Phys.* **30** (1983) 591.
4. B. V. FALKAI, *Makromol. Chemie* **41** (1960) 86.
5. E. HORNBOGEN and K. FRIEDRICH, in "Sonderbände der Praktischen Metallographie", Vol. 9, edited by W. Kopp, H. Bühler (Riederer Verlag, Stuttgart, 1978) p. 143.
6. D. C. BASSETT, "Principles of polymer morphology" (Cambridge University Press, 1981).
7. D. R. NORTON and A. KELLER, *Polymer* **26** (1985) 704.
8. S. A. SALTYKOV, "Stereometrische Analyse" (VEB Deutscher Verlag für Grundstoffindustrie, Leipzig, 1974).
9. R. T. DE HOFF and F. N. RHINES, "Quantitative Microscopy" (McGraw-Hill, New York, 1968).
10. E. E. UNDERWOOD, "Quantitative Stereology" (Addison Wesley, Reading, Massachusetts, 1970).
11. A. RENYI, "Wahrscheinlichkeitsrechnung" (Deutscher Verlag der Wissenschaften, Berlin, 1977).
12. I. N. BRONSTEIN and K. A. SEMENDJAJEW (eds), "Taschenbuch der Mathematik" (Verlag Harri Deutsch, Zürich, 1966).
13. G. E. W. SCHULZE, *Acta. Metall.* **33** (1985) 239.
14. L. O. SCHWAN, L. GRUTESEN and W. WEGER, personal communication.
15. G. E. W. SCHULZE, *J. Crystal Growth* **62** (1983) 7.

*Received 6 May
and accepted 7 December 1988*